doi:10.1246/cl.2012.389
Published on the web March 24, 2012

Y-branched TiO_2 Nanotube Arrays Made by a Simplified Two-step Electrochemical Anodic Oxidation Method

Xu Yang,[1,2] Yi Qu,[1] Yi Fan,[2] and Xingyuan Liu*[2]
[1]*National Key Lab of High Power Semiconductor Lasers, Changchun University of Science and Technology, Changchun 130022, P. R. China*
[2]*State Key Laboratory of Luminescence and Applications, Changchun Institute of Optics, Fine Mechanics and Physics, Chinese Academy of Sciences, Changchun 130033, P. R. China*

(Received January 3, 2012; CL-120004; E-mail: liuxy@ciomp.ac.cn)

Perpendicularly aligned and highly ordered Y-branched TiO_2 nanotube arrays were fabricated by a simplified two-step electrochemical anodic oxidation method via reducing the anodizing voltage. The optimized growth-voltage range is between 28 and 20 V. Different cross-sectional morphologies can be observed when the nanotube arrays are anodized under different voltage ranges. We illustrate here the synthesis process of Y-branched TiO_2 nanotubes and a possible growth mechanism that leads to a variety of tubular branching morphologies.

TiO_2 nanoparticle films with a high surface area are often used as the electron-collecting layer for dye-sensitized solar cells. The large surface area is beneficial to absorb more dye molecules and maximize the amount of photogenerated charge.[1,2] However, the structural disorder of TiO_2 nanoparticle films made of randomly dispersed nanocrystals will enhance scattering of electrons and thus deteriorate charge transport. In recent years, TiO_2 nanotube films have become a powerful candidate because of their ordered and strongly interconnected nanoscale architecture, which can further improve charge separation and charge transport, leading to higher photovoltaic conversion efficiency.[3,4] At present, the methods for preparing TiO_2 nanotubes mainly include template synthesis,[5–7] hydrothermal treatment,[8–10] and anodic oxidation.[11,12] Most common TiO_2 nanotubes represent a straight line morphology. Mohapatra and co-workers in 2008 first showed that Y-branched TiO_2 nanotubes could be prepared on a pure titanium foil by a two-step electrochemical anodic oxidation via increasing the electrolyte temperature.[13] The results showed that Y-branched TiO_2 nanotubes could absorb more visible light than one-dimensional TiO_2 nanotubes of equal thickness. However, only a limited number of Y-branched TiO_2 nanotubes could be obtained by the method of increasing temperature, and defects easily occur on the top of the nanotube arrays.[14] In 2009, Jin et al. showed that Y-branched TiO_2 nanotubes could be prepared by a two-step anodization method via increasing the anodizing voltage in two different kinds of electrolytes.[15] Although it could effectively improve the synthesized quantity of Y-branched TiO_2 nanotubes, this method required two electrolytes in the experiment. In this paper, we will show simplified fabrication of Y-branched TiO_2 nanotube arrays by a two-step anodization method via reducing the anodizing voltage. This method can effectively increase the quantity of Y-branched TiO_2 nanotubes, and two stages of the anodic oxidation process can be completed just in one electrolyte containing NH_4F. The possible growth mechanism of Y-branched TiO_2 nanotubes is discussed. Y-shaped TiO_2 nanotube arrays exhibited a variety of cross-sectional phenomena corresponding to different voltage reduction ranges, such as a low occupancy of Y-shaped nanotubes, interlaminar fracture, and a shrinking waist at the branching location.

Ti foils were degreased ultrasonically in acetone, ethanol, and deionized water for 10 min each and dried by an air stream. A two-electrode configuration was used in the electrochemical anodization, Ti foil was used as the anode, and platinum foil as the cathode. The distance between the electrodes was 1 cm. The electrolyte solution was ethylene glycol containing 0.5 wt % NH_4F and 5 vol % water. All of the anodizations were conducted at 20 °C.

A schematic illustration of four Y-branched TiO_2 nanotube samples fabricated under different voltage ranges is shown in Figure 1. The process started with the preparation of sample (a) on Ti foil by reducing the anodizing voltage. First, the Ti foil was anodized at 26 V for 15 min, then the anodizing voltage was dropped suddenly from 26 V down to 20 V, and the anodization was further continued for 50 min at 20 V to form two-branched nanotubes. At the end of the experiment, the anodized Ti foil was ultrasonically cleaned in deionized water to remove the remnant solution and finally dried in air. After the preparation of sample (a), we further expanded the changing scope of the anodization voltage, such as 28–20, 28.5–20, and 28.9–20 V. The anodization was performed under the same conditions as those in the process of sample (a) except the initial voltage. So we obtained samples (b), (c), and (d) of the Y-branched TiO_2 nanotubes by reduction of the anodizing voltage. The morphology and structure of the Y-branched TiO_2 nanotube samples were characterized using FE-SEM (Hitachi S-4800).

In the two-step anodizing process, we can effectively prepare the Y-branched TiO_2 nanotubes by reducing the anodizing voltage. The anodizing voltage affects not only the growth of the TiO_2 nanotubes directly but also the micromorphologies. The diameter of the TiO_2 nanotubes is linearly proportional to the anodization voltage in every fixed water concentration.[16,17] If we reduce the anodizing voltage, the diameter of the TiO_2 nanotubes will decrease. For sample (a), our anodization

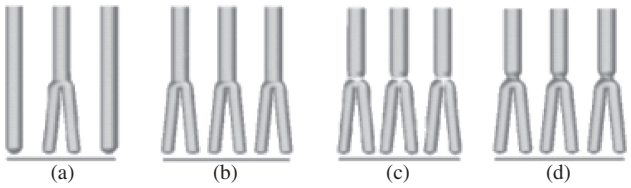

Figure 1. Schematic representation of Y-branched TiO_2 nanotube samples fabricated under different voltage ranges: (a) 26–20, (b) 28–20, (c) 28.5–20, and (d) 28.9–20 V.

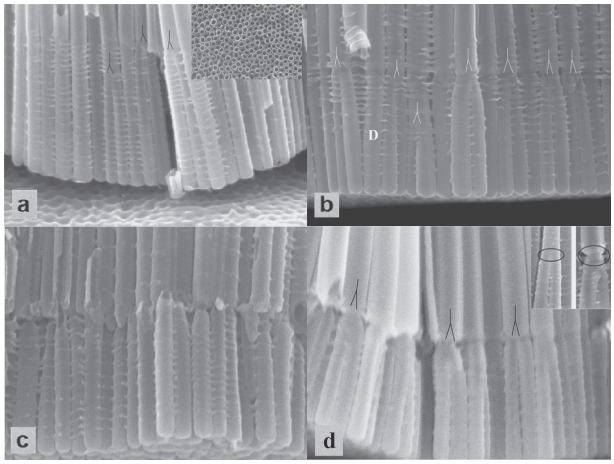

Figure 2. FE-SEM cross-sectional images of Y-branched TiO_2 nanotube samples fabricated by a two-step anodization process under different reduction voltage ranges: (a) 26–20 V, the inset is the top-section view; (b) 28–20; (c) 28.5–20; (d) 28.9–20 V, the inset reveals the differences in the two morphologies in the branched position.

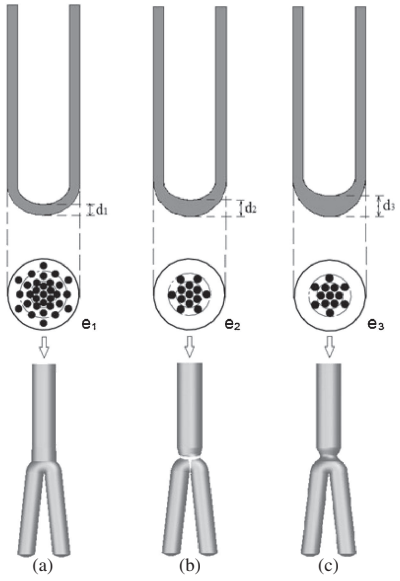

Figure 3. Schematic illustration of a variety of cross-sectional morphologies of Y-branched TiO_2 nanotubes. (a) Y-branched TiO_2 nanotubes with a better morphology fabricated by reducing the anodizing voltage suddenly from 28 to 20 V; (b) Y-branched TiO_2 nanotubes with a fracture morphology in the branched position by reducing the anodizing voltage suddenly from 28.5 to 20 V; (c) Y-branched TiO_2 nanotubes with a shrinking waist morphology in the branched position by reducing the anodizing voltage suddenly from 28.9 to 20 V. d_1, d_2, and d_3 show the oxide thickness at the bottom of the stem nanotubes. e_1, e_2, and e_3 show the selection region of the two core holes for the branched nanotubes.

experiment was performed under reduction of the anodization voltage from 26 to 20 V. As shown in Figure 2a, we can clearly see that two nanotubes with small diameter grow from the bottom of the stem nanotube in branching form. As a result, the "second generation" nanotube arrays grow denser. It is expected that the second generation nanotube arrays have different electronic and photon absorption properties compared with line-shaped TiO_2 nanotube structures. However, we also observed that the quantity of Y-branched TiO_2 nanotubes is limited corresponding to the reduction range of DC voltage, the whole cross-sectional morphology exhibits a phenomenon of a mixture of line-shaped nanotubes and Y-shaped nanotubes. The low occupancy phenomena of the Y-shaped nanotubes were analyzed as follows. First, if a small DC voltage is applied for the initial growth of the stem nanotubes, it will be difficult to cause more oxygen ions to migrate toward the TiO_2/Ti interface for the formation of a thicker oxide barrier layer at the bottom of the stem nanotubes. When the anodizing voltage is reduced suddenly, the formation reaction of the oxide barrier layer will decrease; however, because of a thin oxide barrier layer at the bottom of the stem nanotubes, the formation rate ν_f will only experience a temporary slowdown and will soon reach a new balanced value with a dissolution rate ν_d. At the same time, the fluoride ions in the electrolyte have insufficient time to etch more core holes for the growth of the branched nanotubes. So most of the stem nanotubes will continue to grow, and only a few can form the branched structure.[18] Therefore, if we further shorten the range of the reduction voltage, the Y-branched TiO_2 nanotubes would be more difficult to obtain.

In order to improve the occupation of Y-branched TiO_2 nanotubes, we further expand the reduction range of the anodizing voltage, while maintaining the other anodizing conditions unchanged. For sample (b), the initial anodizing voltage is 28 V for a period of 15 min and then drops down to 20 V for 50 min. As seen in Figure 2b, the occupation of Y-branched TiO_2 nanotubes has been improved greatly. In addition, we notice that part of the line-shaped TiO_2 nanotubes shows a change in topography. For example, for the nanotube D in Figure 2b, the upper section diameter is 95 nm and the lower section is 75 nm. Given that the nanotube diameter is proportional to the voltage and that this diameter can be used as a reference diameter change for other Y-branched TiO_2 nanotubes, we could deduce that this type of line-shaped nanotube corresponds to the Y-branched TiO_2 nanotubes. Just because of the viewing angle, we can only observe the morphology of their profile. Thus, this further implied that the occupation of Y-branched TiO_2 nanotubes has been enhanced.

When the initial anodizing voltage is set to 28.5 V for sample (c), as shown in Figures 2c and 3b, we can obtain two layers of TiO_2 nanotube arrays, but there is a fracturing phenomenon appearing in the branched position. The possible reason for this is as follows. First, the bottom shape of the stem nanotubes is hemispherical. If the oxide barrier layer at the bottom of the stem nanotubes is thin, the electric field distribution can be regarded as relatively uniform. As shown in Figure 3a, the two core holes for the branched nanotubes can be formed anywhere in the selection region at the bottom of the stem nanotubes. The black spots in e_1, e_2, and e_3 of Figure 3 are used to express the honeycomb cells which were etched at the bottom center of stem nanotube by F^- ions. However, the oxide barrier layer at the bottom of stem nanotubes becomes thicker with the increase of the initial anodizing voltage. So the

nonuniformity of the electric field distribution will appear at the hemispherical bottom of the stem nanotubes, and the electric field gradually escalates toward the bottom center of the stem nanotubes. As shown in e_2 of Figure 3b, the selection region of the core holes for the sample (c) begins to shrink. In addition, the core hole enlargement is a very rapid process during nanotube growth. As a result, the core holes are quickly expanded in such a confined space, resulting in the fracture of the nanotube wall in the branched position. However, the position of the core holes still exists, and the growth of these holes under the electric field leads to branched nanotube arrays with small diameter. Finally, we obtained a TiO_2 nanotube array containing two layers of nanotubes with different pore diameters and an interlaminar fracture structure.[19–21]

As shown in Figures 2d and 3c, Y-branched TiO_2 nanotubes with complete morphology can be obtained when the initial anodizing voltage is set to 28.9 V for sample (d). But there is a shrinking waist phenomena in the branching position. Compared with the possible fracture mechanism for sample (c), the common ground is that the two selection regions of the core holes for the branched nanotubes are both decreased (e_2 and e_3 in Figures 3b and 3c). For the Y-branched TiO_2 nanotubes with a shrinking waist phenomena, as the increase of initial anodizing voltage,[22–24] the oxide barrier layer at the stem nanotube bottom of sample (d) was thicker than that of sample (c) ($d_3 > d_2$, as shown in Figures 3b and 3c). The increased thickness in sample (*d*) is beneficial to decrease the rate of core hole enlargement, which will avoid a quick growth in the limited space available at the bottom of the stem nanotubes and prevent the nanotube wall from rupturing. As shown in Figure 2d, we also observe that the stem nanotubes are not immediately branched after suddenly reducing the voltage, and the branching position has moved down. This phenomenon illustrates that the rate of core hole enlargement slowed owing to the increased oxide barrier layer. As a result, the selection region of the core holes for the branched nanotubes decreased at the bottom of the stem nanotubes, the rate of core hole enlargement slowed and the branched position moved down, and as mentioned three factors caused a shrinking waist phenomena of the Y-branched TiO_2 nanotubes.[25]

In summary, we have successfully synthesized Y-branched TiO_2 nanotubes by a two-step electrochemical anodic oxidation via reducing the anodizing voltage in one electrolyte solution. The possible growth mechanism is discussed in this paper. Our results show that a reduction in the voltage range from 28 to 20 V causes better growth of Y-branched TiO_2 nanotubes with better morphology and photoelectric performance. Below or above this voltage range, the Y-branched TiO_2 nanotube arrays will exhibit a variety of cross-sectional phenomena. Understanding the formation mechanism behind these unfamiliar phenomena will be more conducive to predesigning and fabricating high-quality Y-branched TiO_2 nanotube arrays.

This work is supported by the CAS Innovation Program, Jilin Province Science and Technology Research Project No. 20100570, and the National Science Foundation of China grants Nos. 51102228 and 61106057.

References and Notes

1 B. Tan, Y. Wu, *J. Phys. Chem. B* **2006**, *110*, 15932.
2 J. Wang, Z. Lin, *Chem. Mater.* **2010**, *22*, 579.
3 G. K. Mor, K. Shankar, M. Paulose, O. K. Varghese, C. A. Grimes, *Nano Lett.* **2006**, *6*, 215.
4 T. Peng, A. Hasegawa, J. Qiu, K. Hirao, *Chem. Mater.* **2003**, *15*, 2011.
5 W. F. Jiang, Y. H. Ling, S. J. Hao, H. Y. Li, X. De Bai, D. Q. Cang, *Key Eng. Mater.* **2007**, *336–338*, 2200.
6 T. Kasuga, M. Hiramatsu, A. Hoson, T. Sekino, K. Niihara, *Langmuir* **1998**, *14*, 3160.
7 T. Maiyalagan, B. Viswanathan, U. V. Varadaraju, *Bull. Mater. Sci.* **2006**, *29*, 705.
8 J. Yu, H. Yu, B. Cheng, C. Trapalis, *J. Mol. Catal. A: Chem.* **2006**, *249*, 135.
9 L.-Q. Weng, S.-H. Song, S. Hodgson, A. Baker, J. Yu, *J. Eur. Ceram. Soc.* **2006**, *26*, 1405.
10 M.-K. Seo, S.-J. Park, *J. Nanosci. Nanotechnol.* **2011**, *11*, 4633.
11 K. Shankar, G. K. Mor, H. E. Prakasam, S. Yoriya, M. Paulose, O. K. Varghese, C. A. Grimes, *Nanotechnology* **2007**, *18*, 065707.
12 B.-Y. Yu, A. Tsai, S.-P. Tsai, K.-T. Wong, Y. Yang, C.-W. Chu, J.-J. Shyue, *Nanotechnology* **2008**, *19*, 255202.
13 S. K. Mohapatra, M. Misra, V. K. Mahajan, K. S. Raja, *Mater. Lett.* **2008**, *62*, 1772.
14 X. Yang, Y. Qu, Y. Fan, X. Liu, *Sci. China: Phys., Mech. Astron.* **2012**, *55*, 14.
15 Z. Jin, G. T. Fei, X. Y. Hu, S. H. Xu, L. De Zhang, *Chem. Lett.* **2009**, *38*, 288.
16 G. K. Mor, O. K. Varghese, M. Paulose, K. Shankar, C. A. Grimes, *Sol. Energy Mater. Sol. Cells* **2006**, *90*, 2011.
17 H. Yin, H. Liu, W. Z. Shen, *Nanotechnology* **2010**, *21*, 035601.
18 X. Yuan, M. Zheng, L. Ma, W. Shen, *Nanotechnology* **2010**, *21*, 405302.
19 S. W. Ng, F. K. Yam, K. P. Beh, S. S. Tneh, Z. Hassan, *Optoelectron Adv. Mater., Rapid Commun.* **2011**, *5*, 258.
20 C. Shuoshuo, L. Zhiyuan, H. Xing, L. Yi, *J. Mater. Chem.* **2009**, *19*, 5717.
21 S. H. Huh, D. H. Riu, J. Choi, S. J. Kim, E. J. Jin, D. G. Shin, K. Y. Cho, *J. Korean. Phys. Soc.* **2007**, *51*, L1.
22 S. Berger, R. Hahn, P. Roy, P. Schmuki, *Phys. Status Solidi B* **2010**, *247*, 2424.
23 Y. Jo, I. Jung, I. Lee, J. Choi, Y. Tak, *Electrochem. Commun.* **2010**, *12*, 616.
24 A. Valota, D. J. LeClere, P. Skeldon, M. Curioni, T. Hashimoto, S. Berger, J. Kunze, P. Schmuki, G. E. Thompson, *Electrochim. Acta* **2009**, *54*, 4321.
25 Supporting Information is available electronically on the CSJ Journal Web site, http://www.csj.jp/journals/chem-lett/index.html.

